Dry powder formulation of azithromycin for COVID-19 therapeutics

Stefanie Ho Yi Chan, Khalid Sheikh, Mohammed Gulrez Zariwala & Satyanarayana Somavarapu

Published online: 27 Mar 2023.

Submit your article to this journal ☑

Article views: 2491

View related articles ☑

View Crossmark data ☑

Citing articles: 2 View citing articles ☑

Taylor & Francis
Taylor & Francis Group

RESEARCH ARTICLE

Dry powder formulation of azithromycin for COVID-19 therapeutics

Stefanie Ho Yi Chan[a] 🔟, Khalid Sheikh[a], Mohammed Gulrez Zariwala[b] 🔟 and Satyanarayana Somavarapu[a]

[a]Department of Pharmaceutics, UCL School of Pharmacy, London, United Kingdom; [b]Centre for Nutraceuticals, School of Life Sciences, University of Westminster, London, United Kingdom

ABSTRACT

Azithromycin is an antibiotic proposed as a treatment for the coronavirus disease 2019 (COVID-19) due to its immunomodulatory activity. The aim of this study is to develop dry powder formulations of azithromycin-loaded poly(lactic-co-glycolic acid) (PLGA) nanocomposite microparticles for pulmonary delivery to improve the low bioavailability of azithromycin. Double emulsion method was used to produce nanoparticles, which were then spray dried to form nanocomposite microparticles. Encapsulation efficiency and drug loading were analysed, and formulations were characterised by particle size, zeta potential, morphology, crystallinity and in-vitro aerosol dispersion performance. The addition of chitosan changed the neutrally-charged azithromycin only formulation to positively-charged nanoparticles. However, the addition of chitosan also increased the particle size of the formulations. It was observed in the NGI® data that there was an improvement in dispersibility of the chitosan-related formulations. It was demonstrated in this study that all dry powder formulations were able to deliver azithromycin to the deep lung regions, which suggested the potential of using azithromycin via pulmonary drug delivery as an effective method to treat COVID-19.

1. Introduction

First discovered in late 2019, the severe acute respiratory syndrome coronavirus 2 (SARS-CoV-2) has caused a worldwide pandemic – the coronavirus disease 2019 (COVID-19). Since the pandemic first started, there have been several potential treatments in various stages of development. These can be broadly divided into three categories – antivirals (Barnabas et al. 2021, Hung et al. 2020, Rizzardini 2020, ANTICOV 2021, Shoumann et al. 2021, Arnold 2022, Gottlieb et al. 2022, Hammond et al. 2022, Cairns et al. 2022), immune modulators and others involving diverse mechanistic actions (Declercq et al. 2020, Smieszek et al. 2021, Ezer et al. 2021, Mantero et al. 2021, Bramante et al. 2022, Clemency et al. 2022, Profact Inc. 2022, Santoro et al. 2022, Wilkinson et al. 2020). Immune modulators being investigated include azithromycin (Cavalcanti et al. 2020, Furtado et al. 2020, Hinks et al. 2021, Oldenburg et al. 2021), brensocatib (University of Dundee 2021), dexamethasone (The COVID STEROID 2 Trial Group 2021, The RECOVERY Collaborative Group 2021), etesevimab (Eli Lilly and Company 2022, p. 4), otilimab (GlaxoSmithKline 2022), ravulizumab (McEneny-King et al. 2021), risankizumab (National Institute of Allergy and Infectious Diseases (NIAID) 2022) and tofacitinib (Guimarães et al. 2021).

Currently, there are four COVID-19 treatments approved by the Medicines and Healthcare products Regulatory Agency (MHRA) and available within the National Health Service (NHS) – molnupiravir (Lagevrio), nirmatrelvir combined with ritonavir (Paxlovid), remdesivir (Veklury), and sotrovimab (Xevudy) (National Institute for Health and Care Excellence 2022). Molnupiravir, nirmatrelvir combined with ritonavir, and remdesivir are all antivirals, while sotrovimab is an immune modulator. Both molnupiravir and the combination of nirmatrelvir and ritonavir are approved for oral delivery, whereas remdesivir and sotrovimab are delivered intravenously. Pulmonary delivery is also being investigated as an alternative route of administration since COVID-19 affects the respiratory system, and therefore treatments focusing on the lung may be more beneficial (Ruan et al. 2022). The spike protein on the surface of SARS-CoV-2 cells

binds specifically to the cellular receptor target, angiotensin-converting enzyme 2 (ACE2), present on the type 2 pneumocytes in the alveoli in the lungs. As ACE2 is largely present on the mucosal lining of the nose and lungs, it hugely facilitates the entry and infection of the respiratory tract as the host cell proteases cleave the spike protein of SARS-CoV-2. The virus enters the host cell by either endocytosis or direct cell entry through membrane fusion (Kumar *et al.* 2021). There is on-going research on dry powder formulation of remdesivir by various methods, including jet-milling and thin-film freezing (Sahakijpijarn *et al.* 2020, Vartak *et al.* 2021, Ruan *et al.* 2022).

Azithromycin is an antibiotic being used as a treatment for COVID-19 due to its immunomodulatory activity, which decreases production and pro-inflammatory cytokines and inhibits neutrophil activation (Kanoh and Rubin 2010, Echeverría-Esnal *et al.* 2021). *In-vitro* studies and *in-silico* drug screens had suggested azithromycin as a potential candidate against COVID-19 (Touret *et al.* 2020, Oliver and Hinks 2021). However, several clinical trials had found there was no significant difference in efficacy with the use of azithromycin (Cavalcanti *et al.* 2020, Furtado *et al.* 2020, Sekhavati *et al.* 2020). A randomised clinical trial (NCT04332107) suggested that a single dose of oral azithromycin (1.2 g) did not show significant benefits compared to that of placebo at day 14 (Oldenburg *et al.* 2021). Another study (NCT04381962) suggested that the use of oral azithromycin (500 mg once daily orally for 14 days) combined with standard care did not reduce the risk of subsequent hospital admission or death in patients with mild to moderate COVID-19 (Hinks *et al.* 2021). The UK-based RECOVERY trial showed no significant clinical benefit from the use of azithromycin (500 mg by mouth, nasogastric tube, or intravenous injection once a day for 10 days or until discharge, if sooner) for hospitalised patients with severe COVID-19 (Abaleke *et al.* 2021), while the PRINCIPLE trial had found no significant benefit for the routine use of azithromycin (500 mg daily for three days) for reducing recovery time or risk of hospitalisation for people with suspected COVID-19 in the UK community (Butler *et al.* 2021). A possible explanation for the low efficacy might be due to the known issues related to azithromycin's poor pharmacokinetic profile (Lode 1991). Azithromycin has poor gastric stability and a low oral bioavailability of approximately 37%, and its incomplete absorption in blood may account for its relatively poor efficacy (Luke and Foulds 1997). To improve its bioavailability, its solubility and dissolution behaviour need to be increased. This can be done by reducing the particle size to the nanometre range (Müller and Jacobs 2002), which would cause an increase in surface area and augmented dissolution velocity (Keck and Muller 2006).

Delivering azithromycin via the pulmonary route has several advantages over oral drug delivery (Garcia-Contreras and Hickey 2002) – (1) aerosolised azithromycin treats pulmonary infections in a targeted manner without diffusing to other non-specific sites in the body, thus resulting in a high therapeutic concentration locally in the lung, especially in the epithelial lining fluid, with the added benefit of dose reduction (Hickey *et al.* 2006); (2) side effects can be minimised as systemic exposure is minimised, and the drug can also avoid first-pass metabolism (Hayes *et al.* 2010); (3) there is a potential for developing inhaled azithromycin for controlled release systems, hence reducing the frequency of drug administration and increasing patients compliance (Rogueda and Traini 2007); and (4) it can minimise the aerosolisation of lung secretions, thus reducing the risk of spreading the virus to healthcare professionals (Sun 2020). Previous studies had demonstrated the development of inhalable dry powder formulations of azithromycin with other excipients, including co-spray dried azithromycin with mannitol (Li *et al.* 2014a, Young *et al.* 2015) and co-spray dried azithromycin with L-leucine (Mangal *et al.* 2018). Poly(lactic-co-glycolic acid) (PLGA) is a biodegradable polymer that is often used as it is commercially available as well as FDA-approved (Sharma *et al.* 2016). Its drug release rate can be easily modified with the molecular weight of PLGA as well as its polymerisation ratio of lactide to glycolide (Mittal *et al.* 2007, Gentile *et al.* 2014). It can also improve colloidal stability. PLGA decomposes to lactic acid and glycolic acid in the body and is then excreted as CO_2, thus proving it to be safe to use (Danhier *et al.* 2012, Günday Türeli *et al.* 2016). Therefore, this study was aimed at formulating and characterising spray-dried powder of azithromycin-loaded-PLGA nanocomposite microparticles that are suitable for pulmonary drug delivery as an alternative delivery route to promote bioavailability.

High pressure homogenisation is one of the most common methods to produce nanoparticles (Müller and Peters 1998). In order to maximise its effect, double emulsion method was used alongside homogenisation in this study. To avoid particles from aggregating, a surfactant, i.e., PVA, was used to cover the surface of the particles, supporting the electrostatic repulsion and/or steric stabilisation between particles (Grau *et al.* 2000). The emulsion formulated was then lyophilised into powder form to enhance stability (Kocbek *et al.* 2006).

Although there are a lot of advantages of using nanoparticles in dry powder inhalation (DPI) delivery, such as higher drug loading capacity, increased cellular uptake, longer retention and higher chances of mucus penetration, there are several challenges that need to be overcome – (1) prevent aggregation of the particles in inhaler, (2) efficient redispersion of drug in lung fluid, (3) maintaining the particles in dry state until delivery, and (4) preservation of the particles and the corresponding biological activity of the drug throughout manufacturing stages. Therefore, particle engineering is introduced to produce particles of desired characteristics with lesser expense (Han *et al.* 2002). Commonly used particle engineering techniques include (1) make of large hollow nanoparticles for deep lung deposition, (2) make of effervescent particles to improve dispersion, (3) surface modification to improve nanoparticle characteristics as a delivery vehicle, and (4) encapsulating nanoparticles within microparticles to prevent particle aggregation.

2. Materials and methods

2.1. Materials

Azithromycin dihydrate (AZI), $C_{38}H_{72}N_2O_{12}\cdot 2H_2O$ (Tokyo Chemical Industry Co. Ltd) was used as the drug under investigation. Poly(vinyl alcohol), 87–89% hydrolysed from Sigma-Aldrich (Dorset, U.K.) was used as surfactant. Poly(D,L-Lactide-Co-Glycolide) crystals of ratio 50:50 were purchased from Alkermes plc (Ohio, U.S.A). Chitosan oligosaccharide lactate was purchased from Sigma-Aldrich (Dorset, U.K.). Potassium dihydrogen orthophosphate and sodium hydroxide were purchased from Fisher Scientific Ltd. (Loughborough, U.K.). HPLC grade methanol and dichloromethane were purchased from Fisher Scientific Ltd. (Loughborough, U.K.) and Sigma-Aldrich (Dorset, U.K.) respectively.

2.2. Methods

2.2.1. Preparation of azithromycin-loaded-PLGA nanoparticles by double emulsion method

Azithromycin dihydrate-loaded 50:50 poly(lactic-co-glycolic acid) (PLGA) nanoparticles were prepared by double emulsion method. 100 mg of PLGA and 10 mg of azithromycin dihydrate were dissolved in 10 ml of dichloromethane (DCM). 1 ml of 2% polyvinyl alcohol (PVA) solution was then added. This solution was emulsified for two minutes using a homogeniser (IKA Ultra-Turrax T-25 Digital Homogeniser) with 24,000 rpm to form the primary emulsion. This primary emulsion was added into 25 ml of the 0.5% PVA solution (for azithromycin only formulation) or 12.5 ml of 0.5% PVA solution and 12.5 ml of 0.1% chitosan oligosaccharide lactate solution (for azithromycin and chitosan formulation), and then emulsified by a homogeniser for five minutes. This secondary emulsion was then homogenised with a diluted (0.1%) PVA solution for a further five minutes. The emulsion was then left to stir at a temperature range of 40 °C – 45 °C for up to four hours to remove the solvent. Blank nanoparticles were prepared under the same conditions but with absence of the drug. For optimisation purposes, three different types of chitosan, i.e., chitooligosaccharide (CO), chitosan hydrochloride (CH), chitosan oligosaccharide lactate (COL), were used; and COL was chosen to be used in the formulations presented in this study.

2.2.2. Characterisation of azithromycin-loaded-PLGA nanoparticles
2.2.2.1. Particle size and zeta potential measurement by dynamic light scattering (DLS).
The size distribution and zeta potential of nanoparticles were obtained as Z_{Ave} hydrodynamic diameter, polydispersity index (PDI) and zeta potential (§) using Zetasizer Nano ZS (Malvern Instruments, UK). 1 ml of the sample was pipetted directly into the zeta potential DTS1070 folded capillary cell (Malvern Panalytical, UK). Samples that were measured after filtration were filtered with a 0.45 µm filter membrane. Zeta potential was calculated from electrophoretic mobility using the Helmholtz-Smoluchowski equation by the Malvern data analysis software. Measurements were performed three times; the mean value and standard deviation (SD) of the particle size, PDI and zeta potential were then calculated.

2.2.2.2. Encapsulation efficiency and drug loading by high-performance liquid chromatography (HPLC).
Samples were placed in a centrifuge tube (size: 14 ml) and centrifuged at 9500 rpm (angle rotor 19777-H) for 30 min at 4 °C in a refrigerated centrifuge (Sigma Laborzentrifugen, Germany). The supernatants were then extracted and injected into high-performance liquid chromatography (HPLC) vials ready for analysis. HPLC with UV/Vis detector (Agilent 1200 Series, USA) at wavelength 205 nm was used to quantify azithromycin dihydrate in preparations, using a validated method with minor modifications (Al-Rimawi and Kharoaf 2010). The analytical column, C18 reversed-phase 250×4.6 mm was selected as the stationary phase. Separation was carried out using a mobile phase 90:10 (by volume) of methanol and

buffer of pH 7.54 [Phosphate buffer was prepared by dissolving 4.50 g of potassium dihydrogen orthophosphate in 1000 ml of water (0.3 M), adjusted to pH 7.54 with 10% sodium hydroxide solution]. The injection volume used was 20 μL at 1 ml/min flowrate.

Encapsulation efficiency was calculated from Equation (1) while drug loading was calculated using Equation (2).

$$\text{Entrapment efficiency (\%)}$$
$$= \frac{(\text{Total concentration of AZI} - \text{Concentration of unentrapped AZI})}{\text{Total concentration of AZI}} \times 100\%$$
$$[1]$$

$$\text{Drug loading (\%)}$$
$$= \frac{\text{Total weight of entrapped azithromycin}}{\text{Total weight of all raw materials used}} \times 100\%$$
$$[2]$$

2.2.2.3. Morphology of nanoparticles by transmission electron microscopy (TEM).
The morphology of the nanoparticles was determined using transmission electron microscopy (TEM; Philips/FEI CM120 Bio Twin, FEI Netherlands). Samples were placed on copper grids for viewing and excess droplets were wicked away with filter paper. After two minutes, a drop of 1% phosphotungstic acid was placed onto the copper grid for negative staining. The grid was dried at room temperature and observed using TEM.

2.2.3. Preparation of azithromycin-loaded-PLGA nanocomposite microparticles by spray drying
50 ml of all four nanocomposite formulations (azithromycin formulation without centrifugation, azithromycin formulation with centrifugation, azithromycin and chitosan formulation without centrifugation, and azithromycin and chitosan formulation with centrifugation) were spray dried using a mini laboratory spray dryer, model B-290 (Büchi Labortechnik, Switzerland) in an open-loop mode configuration using compressed air as the drying gas. For the two formulations that required centrifugation, formulations were placed in a centrifuge tube (size: 50 ml) and centrifuged at 9500 rpm (angle rotor 19776-H) for 30 min at 4 °C in a refrigerated centrifuge (Sigma Laborzentrifugen, Germany) prior to spray drying. The spray drying process was done under the following conditions: inlet temperature (T_{in}) at 120 °C, corresponding to an outlet temperature (T_{out}) at 42 °C; aspirator rate at 50%; spray gas flow: 536 L/h, pump rate at 5%. The spray-dried powder was then collected from several vessels of the spray dryer.

2.2.4. Characterisation of azithromycin-loaded-PLGA nanocomposite nanoparticles
2.2.4.1. Yield and quality of formulations.
The yield of the spray-dried formulations were accurately weighed using an electronic weighing scale and the appearance of the formulations were documented.

2.2.4.2. Morphology of nanocomposite microparticles by scanning electron microscopy (SEM).
Scanning electron microscopy (SEM) was used to examine the surface morphology of produced powders. Samples were prepared by placing a small amount of freshly prepared spray-dried powder on to 12.5 mm aluminium specimen pin stubs covered with double-sided adhesive black carbon tabs (Agor Scientific, UK). The sample was sputter-coated with gold (Quorum Q150R; Quorum Technologies Ltd., Sussex, UK) prior to observation under SEM (FEI Quanta 200 F SEM; FEI, Eindhoven, Netherlands) at an acceleration voltage of 5 kV.

2.2.4.3. Particle size by laser diffraction analysis (LDA).
The particle size distribution of the powder was determined using a Sympatec HELOS BF laser diffraction analyser (Sympatec GmbH, Clausthal-Zellerfeld, Germany) with RODOS/M dry powder disperser. The sample was loaded into a sealed sample tube and the tube was inserted into the micro-dosing device – ASPIROS. Sufficient sample was loaded to obtain an obscuration of >1 and each sample was measured in triplicate at an air pressure of 4 bar. Results were analysed using Windox 5 (version 5.7.0.0) software.

Results were analysed based on Mie Evaluation Extended (MIEE) algorithm for spherical, isotropic and homogenous particles, which transferred the scattered light data into particle size information. The complex refractive index value used in the analysis was 1.550, with air as continuous phase. Results were expressed as the volume mean particle size and percentage undersize at 10% (X_{10}), 50% (X_{50}) and 90% (X_{90}) and volume mean diameter (VMD).

VMD is the first moment of a $q_3(x)$ (particle volume over particle size) distribution and was calculated as follows. (Ref: ISO 9276–2:2014 Representation of results of particle size analysis—Part 2: Calculation of average particle sizes/diameters and moments from particle size distributions)

$$\text{VMD} = M_{1,3} = \sum_{i-1}^{n} \bar{x}_i \cdot q_3(\bar{x}_i) \cdot (x_{u,i} - x_{l,i}) \quad [3]$$

(where n = number of particle size intervals, $\bar{x}_i$ = arithmetic mean value of particle size interval i, $x_{u,i}$ = upper limit of particle size interval i, $x_{l,i}$ = lower limit of particle size interval i)

The width of distribution was expressed as Span according to the following equation:

$$\text{Span} = (X_{90} - X_{10})/X_{50} \qquad [4]$$

2.2.4.4. Fourier-transform infra-red spectroscopy (FTIR).
FTIR analysis was undertaken using a Spectrum 100 FTIR spectrometer (Perkin Elmer, Massachusetts, USA). Spectra were recorded over the range 4000–650 cm^{-1} with a resolution of 4 cm^{-1} and scanning speed of 0.2 cm/s.

2.2.4.5. Differential scanning calorimetry (DSC).
Thermal analysis was performed on accurately weighed 5 mg samples using hermetically sealed aluminium pans (Tzero pans), a Q series^{TM} DSC auto-sampler and TA DSC Q2000 (TA instruments-Waters LLC, New Castle, DE, USA). The melting point (T_m) of samples was recorded under a 20 ml/min dry nitrogen gas purge at a flow rate of 50 ml/min. The samples were heated at a rate of 10 °C/min from 20 °C to 120 °C to remove any water particles, then they were equilibrated at 20 °C before being heated at a rate of 10 °C/min from 20 °C to 300 °C. Calibration of the instrument was performed routinely using indium as the calibrant.

2.2.4.6. X-ray powder diffraction (XRD).
XRD analysis of samples was performed using Rigaku Mini-Flex 600 (Rigaku, Tokyo, Japan). X-ray tube was operated at a generator voltage of 40 kV and a current of 15 mA. Diffraction patterns were recorded over diffraction angle (2θ) of 3°–60°, a scanning rate of 5°(2θ)/min and scan step of 0.05° (2θ).

2.2.4.7. In-vitro aerosol dispersion performance by Next Generation Impactor (NGI®).
The aerosol properties of the dry powders were evaluated using the NGI® (Copley Scientific Limited, Nottingham, UK) conducted under pharmacopoeial conditions (Apparatus E, European Pharmacopoeis, Chapter 2.9.18). Air flow through the apparatus was adjusted to be at 60 ± 3 L/min using vacuum pump and two-way solenoid valve timer. The air flow rate was tested using a flow metre (DFM2000, Copley Scientific Limited, Nottingham, UK) prior to the testing.

The central cup of the pre-separator insert was filled with 15 ml of methanol and the impaction cups were coated with 1% v/v silicone oil in hexane before analysis. Powder samples (20 ± 1 mg) were accurately weighed and filled into no. 3 hard gelatine capsules and were individually loaded into the dosage chamber of an Aerolizer® device (Novartis, Surrey, UK). The capsule was pierced and the Aerolizer® was inserted into a mouth-piece adaptor. The powder was drawn into the NGI® and tested for 4s at 60 L/min. This was carried out using three capsules for each sample. After all three actuations, powder in capsules, device, mouth-piece, induction port, and stages 1–8 of the NGI® were collected with thorough rinsing using methanol into separate volumetric flasks. The solutions were mixed in a bath sonicator for one hour and left at room temperature overnight to allow azithromycin to be fully dissolved in methanol prior to azithromycin determination using HPLC.

Under these conditions, the cut-off diameter according to Apparatus E, European Pharmacopoeia, Chapter 2.9.18 for each NGI® stage are as follows:

Stage 1: 8.06 µm, Stage 2: 4.46 µm, Stage 3: 2.82 µm, Stage 4: 1.66 µm, Stage 5: 0.94 µm, Stage 6: 0.55 µm, Stage 7: 0.34 µm and Stage 8 as terminal Micro-Orifice Collector (MOC)

The aerosolisation parameters, including fraction recovered (FR), emitted dose (ED), fine particle dose (FPD) and fine particle fraction (FPF) were calculated as follows:

$$FR = \frac{\text{Mass of azithromycin from capsule to Stage 8}}{\text{Initial mass of azithromycin loaded into the capsule}} \times 100\%$$
$$[5]$$

$$ED = \frac{\text{Mass of azithromycin from device to Stage 8}}{\text{Mass of azithromycin from capsule to Stage 8}} \times 100\%$$
$$[6]$$

$$FPD = \text{Mass of azithromycin on Stage 2 to Stage 8}$$
$$[7]$$

$$FPF = \frac{\text{Fine particle dose}}{\text{Initial mass of azithromycin loaded into the capsule}} \times 100\%$$
$$[8]$$

Mass median aerodynamic diameter (MMAD) is determined as particle size at the 50% of cumulative fraction by mass for the aerosolised powders. It was calculated from the graph of cumulative fraction against effective cut-off diameter on log probability axes. Geometric standard deviation (GSD) is a measure of the width of an aerodynamic particle size distribution. It was calculated using the same plot as for calculation of MMAD using following formula:

$$\text{GSD} = (d_{84}/d_{16})^{1/2} \qquad [9]$$

2.2.5. Statistical analysis
One-way ANOVA statistical analysis was carried out using IBM SPSS Statistics Data Editor. The sum of squares, df, mean square, F-value and p values were determined by the programme. For all analyses, differences were considered statistically significant when $p \leq 0.05$.

3. Results and discussion

3.1. Preparation of azithromycin-loaded-PLGA nanoparticles by double emulsion method

Particle size was the first-line parameter used to determine which formulation(s) should be formulated as a dry powder for pulmonary drug delivery at a later stage. Different processes such as filtration, increasing PVA concentration in the primary emulsion, volume of DCM used in the organic phase, ultrasonic disruption, duration of the homogenisation process and the inclusion of dilution phase were carried out to optimise the particle size. In general, it was observed that the longer the homogenisation process in the dilution phase, the smaller the particle size; and that the larger the ratio of secondary emulsion to dilution phase, the larger the particle size.

PLGA 50:50 ratio of lactic and glycolic acid was used as it was proved to have faster hydrolytic activities than those of other ratios (Gentile *et al*. 2014, Mittal *et al*. 2007). However, the surface of PLGA nanoparticles is believed to be negatively-charged, which might affect the mucosal adsorption. Therefore, in this study chitosan was also used, aiming to modify the surface charge of the nanoparticles (Dasankoppa *et al*. 2017). The physiochemical properties of chitosan are dependent on its degree of polymerisation, average molecular weight and the degree of deacetylation, hence different types of chitosan have different physiochemical properties. Three different types of chitosan, i.e., chitooligosaccharide (CO), chitosan hydrochloride (CH), chitosan oligosaccharide lactate (COL), were used for optimisation. CO was first used, however the zeta potential obtained was not as high as desired even the concentration of CO was 1.6%. In both CH and COL, it was observed that both the particle size and surface charge increased as the concentration of chitosan increased. This contradicted data presented by Perez *et al*. and Lertsutthiwong *et al*, who previously suggested that zeta potential and/or surface charge were not dependent on the nature of the active substance, concentration of polymer or stabiliser (Perez *et al*. 2001).

3.2. Characterisation of azithromycin-loaded-PLGA nanoparticles

3.2.1. Particle size and zeta potential measurement by dynamic light scattering (DLS)

Both formulations were proven to be monodisperse/uniform as the PDI obtained were greater than 0.2, ranging from 0.4 to 0.6. However, the addition of chitosan increased the particle size of the formulation. It was demonstrated in this study that the addition of chitosan altered the neutrally-charged drug formulations to positively-charged nanoparticles. Previous studies also proved the electrostatic interaction between positively-charged chitosan and neutrally-charged or negatively-charged nanoparticles (Fonte *et al*. 2011).

Formulation which contained chitosan was positively-charged, hence this electrostatic charge on the particles will induce an opposing charge on the walls of the respiratory tract, which results in attraction between particles and walls, potentially causing the formulations to stay exactly where they are delivered on the lung. In addition, chitosan can also possibly be used as the matrix for controlled drug delivery system. Therefore, the use of chitosan could potentially enhance adhesion performance, resulting in increased bioavailability as well as improving the elongated duration of drug release, thus making it effective for treating local diseases over a prolonged time and improve patients' compliance with reduced dosage.

3.2.2. Encapsulation efficiency and drug loading by ultraviolet-visible spectroscopy (UV-Vis) and high-performance liquid chromatography (HPLC)

As stated in Table 1, drug-only formulation showed a higher encapsulation efficiency than chitosan-related formulation. Interestingly, the order of drug loading was in reverse order of encapsulation efficiency, with chitosan-related formulation having a higher drug loading.

3.2.3. Morphology of nanoparticles by transmission electron microscopy (TEM)

From the TEM images (Figure 1), it can be concluded that the nanoparticles formed in both formulations were spherical and that demonstrated a nano-range particle size.

3.3. Preparation of azithromycin-loaded-PLGA nanocomposite microparticles by spray drying

By optimising parameters such as aspirator rate, air humidity, inlet temperature, spray air flow, pump rate, concentration, etc., can cause an impact in areas like outlet temperature, particle size, yield and humidity of final product. In most cases, a general trend is observed in correlation between these parameters and the quality of final product, e.g., increasing aspirator rate will result in increasing humidity as well as yield. However, there is one

Table 1. Mean particle size, polydispersity index (PDI), zeta potential, encapsulation efficiency and drug loading of the two formulations (mean ± SD, $n = 3$).

Formulation name	Particle size (nm)	PDI	Zeta potential (mV)	Encapsulation efficiency (%)	Drug loading (%)
Azithromycin with 2% PVA solution as primary emulsion, 0.5% PVA as secondary emulsion and 0.1% PVA as dilution phase (D/2.0P/0.5P/0.1P)	464.48 ± 19.85	0.60 ± 0.04	−1.38 ± 0.12	90.62 ± 0.31	3.24 ± 0.01
Azithromycin with 2% PVA solution as primary emulsion, 0.5% PVA and 0.1% COL as secondary emulsion and 0.1% PVA as dilution phase (D/2.0P/0.5P0.1COL/0.1P)	639.03 ± 14.79	0.40 ± 0.01	29.0 ± 0.52	85.86 ± 0.33	3.73 ± 0.01
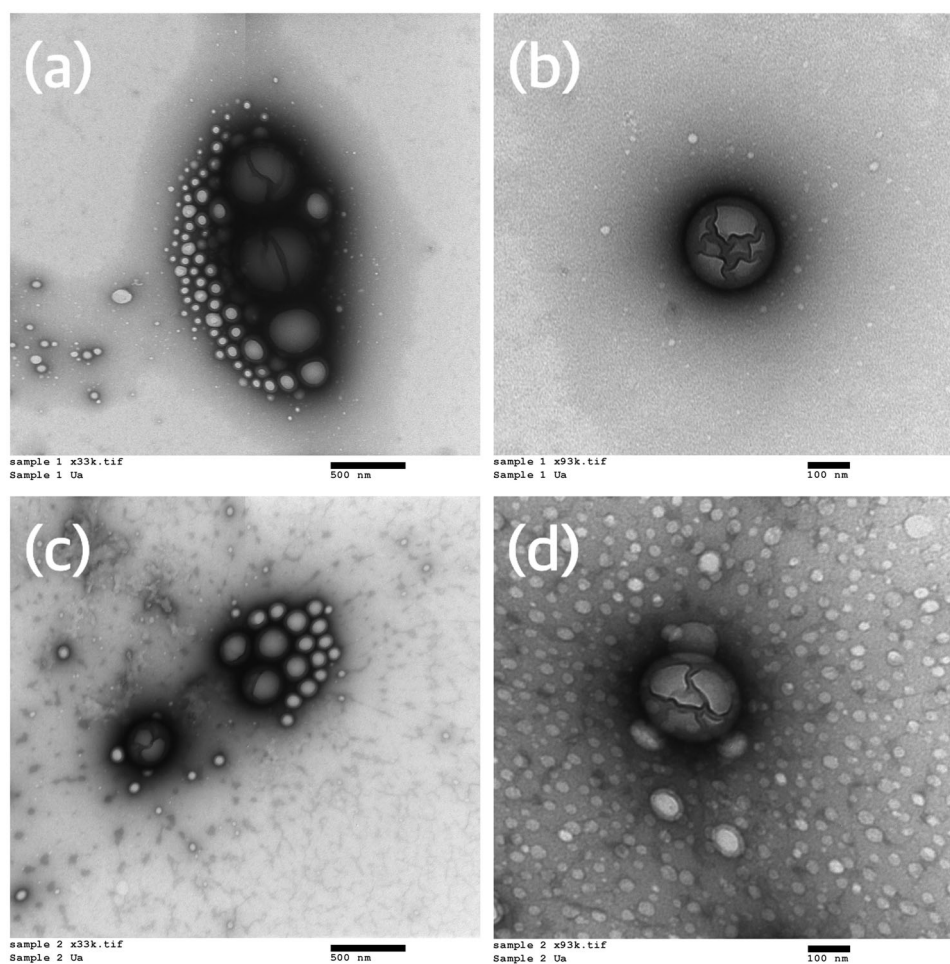
Figure 1. Transmission electron micrographs of nanoparticles of the final two formulations – (a) azithromycin formulation (33,000× magnification), (b) azithromycin formulation (93,000× magnification), (c) azithromycin and chitosan formulation (33,000× magnification), (d) azithromycin and chitosan formulation (93,000× magnification).

parameter dependent on the application, i.e., the relationship between pump rate and the yield obtained. Therefore, in this study, four pump rates were used for optimisation and the one which produced the highest yield was used to spray dry the remaining formulations.

Pump rates of 5%, 10%, 15%, and 25% were used to spray dry azithromycin formulation without centrifugation. The percentage yields of formulations developed for 5%, 10%, and 15% pump rate were 55.5%, 48.6%, and 43.8% respectively. Liquid was formed instead of powder with the pump rate of 25%. As 5% pump rate produced the

highest yield, this was used to spray dry the remaining formulations.

3.4. Characterisation of azithromycin-loaded-PLGA nanocomposite nanoparticles

3.4.1. Yield and quality of formulations

White powders were formed for all four formulations. The mean yield ($n = 3$) of azithromycin formulation without centrifugation (AZI w/o) and azithromycin and chitosan formulation without centrifugation (A&C w/o) were 152.12 ± 17.34 mg and 134.63 ± 15.23 mg respectively, while the mean yield ($n = 3$) of azithromycin formulation with centrifugation (AZI w/) and azithromycin and chitosan formulation with centrifugation (A&C w/) were 29.94 ± 8.75 mg and 43.31 ± 6.54 mg respectively. It was shown that the yield of formulations without centrifugation were at least 3-fold than that of its corresponding formulation with centrifugation. The difference in mass was deduced to be the mass of excessive PVA and/or chitosan that were present in the supernatants.

3.4.2. Morphology of nanocomposite microparticles by scanning electron microscopy (SEM)

The micrographs (Figure 2) showed that all four formulations were spherical shaped with smooth and spongy surface morphology. Spherical particles were believed to have decreased contact area which then lead to a reduction in cohesiveness as well as enhancement in both dispersibility and aerosolisation (Hassan and Lau 2009). It was shown that the two formulations without centrifugation (Figure 2(a,b,e,f)) had a relatively smoother surface, suggesting the excess PVA in the supernatants acted as an external layer to cover the particles and as a surfactant to prevent particles from aggregating, hence a lower particle size. The micrographs for the formulations with centrifugation provided more insight as to how the nanocomposite particles were packed together to form microparticles, as shown in Figure 2(c,d,g,h). In terms of smoothness, AZI w/o appeared to be the smoothest, followed by A&C w/o, AZI w/ and A&C w/. This indicated that centrifugation effectively made the particles surface less smooth and corrugated, and that chitosan also produced the same effect, explaining why A&C w/ had the roughest and most corrugated surface. From previous studies, it was shown that corrugations on the surface of particles further decreased the contact area between particles and their cohesiveness while increasing dispersibility (Bandyopadhyaya et al. 2004). This finding was in good agreement with

the formulations' in-vitro aerosol dispersion performance by NGI®.

3.4.3. Particle size by laser diffraction analysis (LDA)

The laser sizing data of all the spray-dried formulations were summarised in Table 2. A uni-modal size distribution was demonstrated across all four formulations. The span values of all formulations were between 1.583 and 1.758, which proved a narrow size distribution. The X_{50} for all spray-dried powders were between 2.773 µm and 3.843 µm, which proved them to be suitable candidates for pulmonary drug delivery.

It was also observed that the particle sizes of formulations with centrifugation were larger than that of without centrifugation. Besides, the particle sizes of chitosan-related formulations were larger than that of drug-only formulations, which were consistent with the result when they were formulated as nanoparticles.

3.4.4. Fourier-transform infra-red spectroscopy (FTIR)

From Figure 3, it was observed that the two formulations without centrifugation shared a similar IR spectrum as PVA and/or chitosan, with the additional peaks at 1754 cm^{-1}, which was originated from PLGA and azithromycin. However, intensity was not as high as their raw materials. Besides, the absorption bands at 2997 cm^{-1} and 2948 cm^{-1}, corresponding to PLGA, disappeared in these two formulations, showing the dominant presence of PVA. From Figure 3, it was observed that the two formulations with centrifugation shared an identical IR spectrum as PLGA, including same intensity of peaks. This suggested that the dominant presence of PVA in the other two formulations were reduced after centrifugation and the removal of supernatant, which then led to PLGA exerting a greater impact on these two structures.

3.4.5. Differential scanning calorimetry (DSC)

All the samples were first heated up to 120 °C to remove any water molecules present in the samples. One endothermic peak was observed in the DSC thermograms of azithromycin and COL at 126.08 °C and 224.40 °C respectively (Figure 4). These two peaks both indicated melting instead of dehydration, as water was already removed in the first cycle as mentioned. According to literature, the melting point of azithromycin dihydrate is 126 °C which corresponds with the data obtained in this study. It was also noted that there was a tiny, broad glass transition at
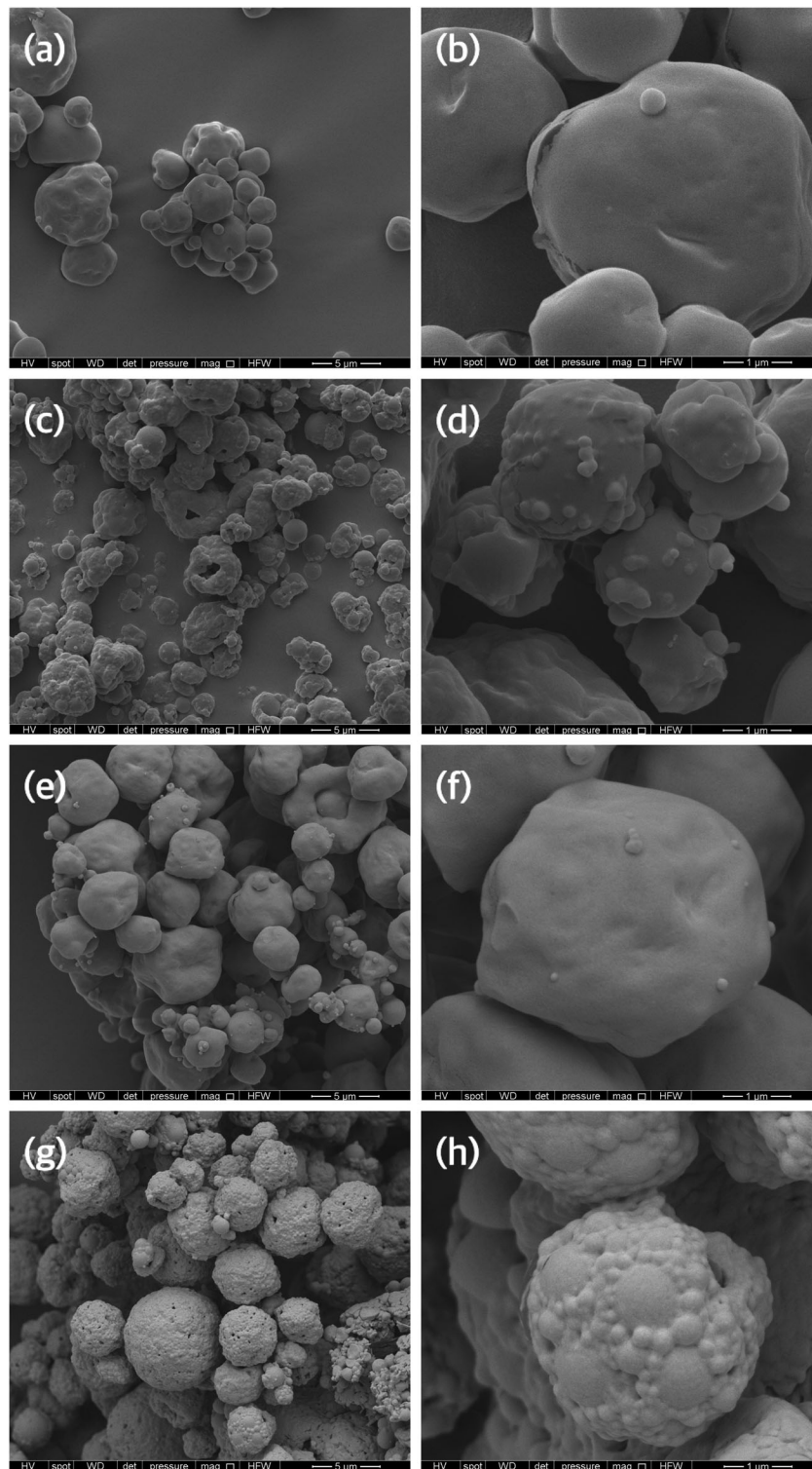
Figure 2. Scanning electron micrographs of spray-dried formulations – (a) azithromycin formulation without centrifugation (10,000× magnification), (b) azithromycin formulation without centrifugation (50,000× magnification), (c) azithromycin formulation with centrifugation (10,000× magnification), (d) azithromycin formulation with centrifugation (50,000× magnification), (e) azithromycin and chitosan formulation without centrifugation (10,000× magnification), (f) azithromycin and chitosan formulation without centrifugation (50,000× magnification), (g) azithromycin and chitosan formulation with centrifugation (10,000× magnification), (h) azithromycin and chitosan formulation with centrifugation (50,000 × magnification).

Table 2. X_{10}, X_{50}, X_{90}, VMD and Span value of all four formulations (mean $\pm$ SD, $n = 3$).

Formulation name	X_{10} (μm)	X_{50} (μm)	X_{90} (μm)	VMD (μm)	Span
AZI w/o	1.06 ± 0.03	2.77 ± 0.19	5.70 ± 0.26	3.50 ± 0.42	1.68 ± 0.10
AZI w/	1.40 ± 0.07	3.46 ± 0.21	7.29 ± 0.35	5.56 ± 0.25	1.71 ± 0.22
A&C w/o	1.11 ± 0.02	3.59 ± 0.28	7.39 ± 0.15	4.78 ± 0.18	1.76 ± 0.11
A&C w/	1.56 ± 0.03	3.84 ± 0.10	7.64 ± 0.22	5.69 ± 0.27	1.58 ± 0.10
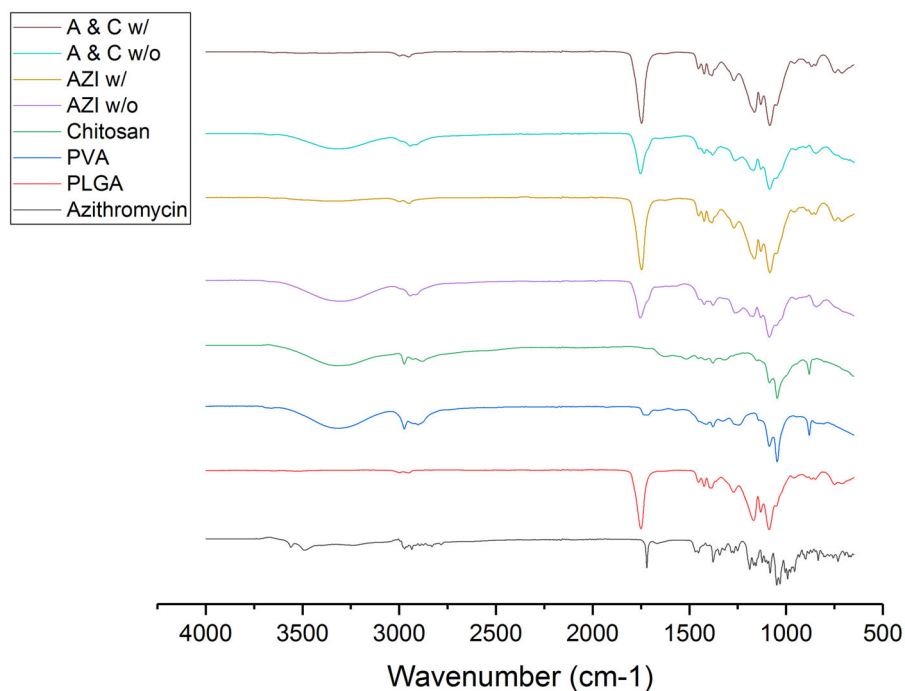
Figure 3. FTIR spectrum of all raw materials and the four spray-dried formulations.
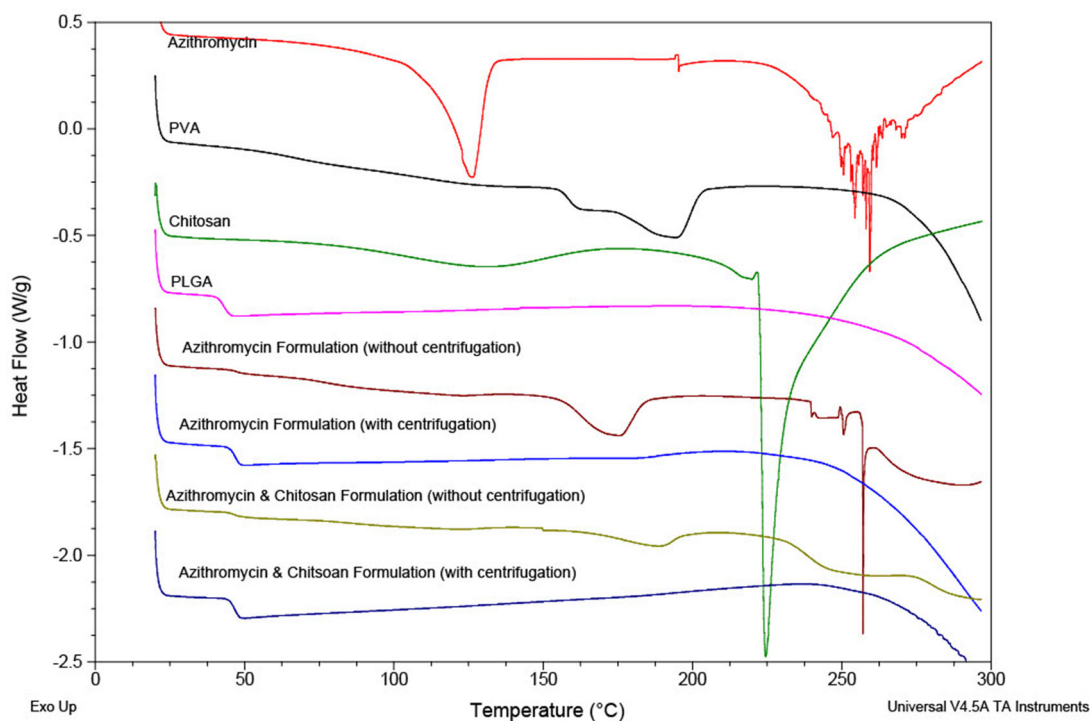
Figure 4. DSC spectrum of all raw materials and the four spray-dried formulations.
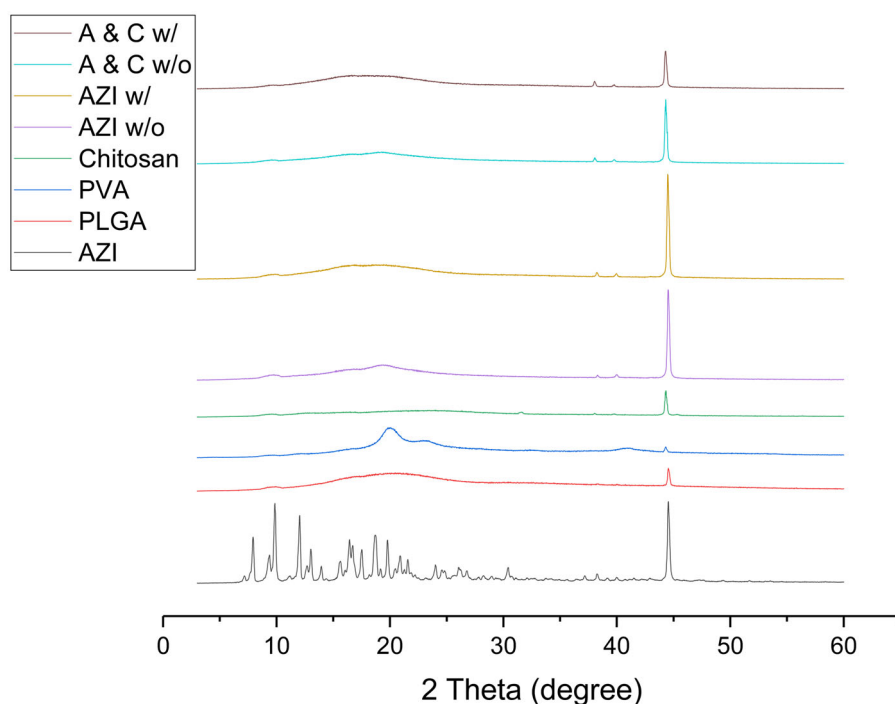
Figure 5. XRD spectrum of all raw materials and the four spray-dried formulations.

Table 3. Aerodynamic parameters of formulations delivered to the NGI® (mean ± SD, $n = 3$).

Formulation name	Fraction recovered (%)	Emitted dose (%)	FPF (%)	MMAD (μm)	GSD
AZI w/o	62.53 ± 2.77	80.14 ± 4.30	41.49 ± 5.86	4.14 ± 0.20	1.86 ± 0.20
AZI w/	71.68 ± 2.99	88.06 ± 5.63	56.02 ± 2.03	4.03 ± 0.26	1.74 ± 0.04
A&C w/o	70.43 ± 2.32	81.28 ± 10.36	48.21 ± 10.22	4.02 ± 0.32	1.83 ± 0.25
A&C w/	71.48 ± 5.18	91.61 ± 1.67	60.42 ± 6.19	4.21 ± 0.31	1.78 ± 0.09

~127 °C, thus suggesting COL might be slightly amorphous as well. For PLGA, there was evidence of glass transition temperature at 42.99 °C. As for PVA, both behaviours were observed in the thermogram – a glass transition at 158.41 °C and an endothermic peak indicating melting at 192.88 °C. From the thermogram, it can be concluded that azithromycin was crystalline, COL to a large extent was crystalline and that PLGA was amorphous. As for PVA, since it possessed both behaviours, it was of a semi-crystalline and semi-amorphous structure. The structure of the two formulations without centrifugation were similar to that of PVA, while the other two formulations with centrifugation were similar to that of PLGA, thus showing they were of a crystallinity similar to PVA and PLGA respectively.

A broad, asymmetric peak was observed in Formulation AZI w/o and Formulation A&C w/o at 174.17 °C and 188.33 °C respectively, thus indicating they were crystalline but impure as expected as they were of a formulation of multiple compounds. Glass transition was observed in Formulation AZI w/ and Formulation A&C w/ at 46.46 °C and 46.19 °C

respectively, thus indicating they were of amorphous structures.

Since the formulations with centrifugation showed no signal of PVA, it can be deduced that by removing the supernatants after centrifugation and redissolving the pellets in water for spray drying had successfully removed the excess PVA in the formulation, and that the presence of excessive PVA overshadowed the effect of PLGA in the two formulations without centrifugation. This possibly explained why the yield of formulations without centrifugation were higher than that without, as this could be most likely due to the presence of excessive PVA. Moreover, it was deduced that azithromycin and/or chitosan were fully encapsulated within PLGA (carrier) as no corresponding peaks of azithromycin and/or COL were shown in the DSC spectrum of all the formulations. If chitosan was fully encapsulated as deduced, then the stability issue in the nanoparticles formulation was solved by spray drying the formulation. As seen in the thermograms of physical mixture of azithromycin and PLGA of ratio 1:1, their corresponding melting peak or glass transition were observed. However, in the thermograms of physical
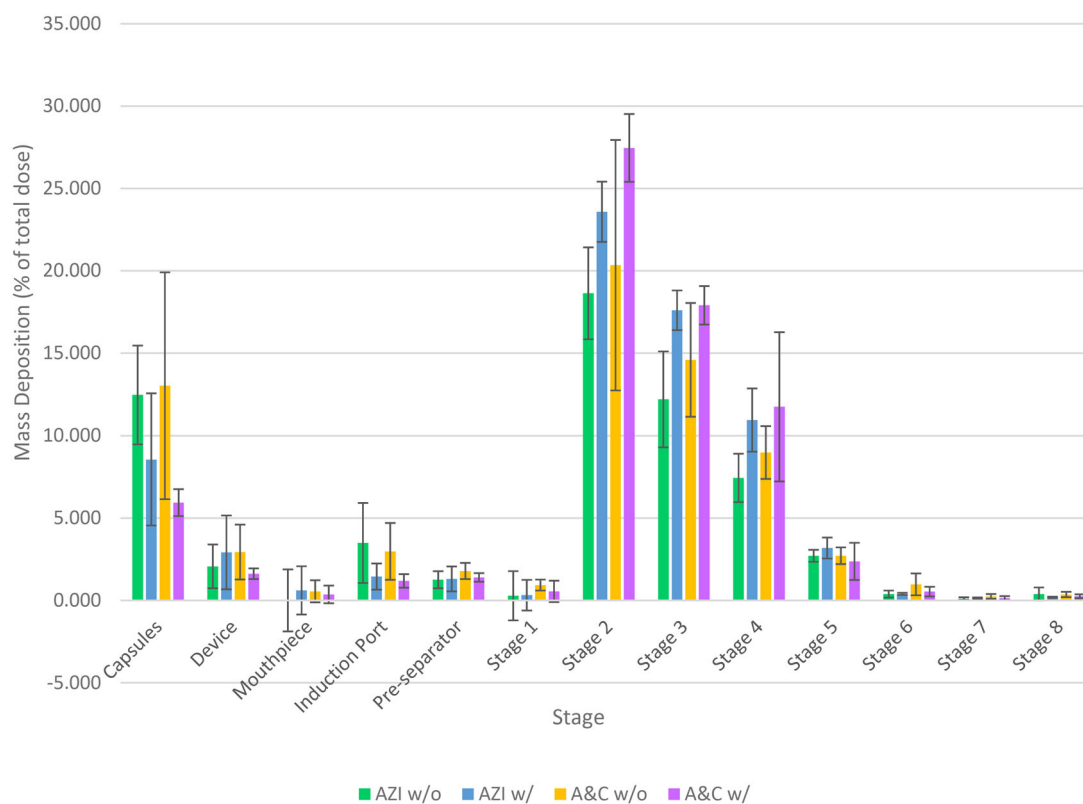
Figure 6. NGI® deposition profile of all four formulations.

mixture of azithromycin and PLGA of ratio 1:10, which was the actual ratio used in all formulations, only glass transition of PLGA was observed, there was no sign of azithromycin. Therefore, besides the possibility that azithromycin was fully encapsulated/dispersed uniformly within the carrier in all formulations, it can also be that the amount of drug present was lower than that of the detection limit, so no peak of azithromycin was recorded.

As Formulation AZI w/ and Formulation A&C w/ had a higher glass transition temperature than that of PLGA, it indicated that it was less amorphous, because the more amorphous the structure is, the easier the molecules inside can move around to break out of the rigid glassy state to the soft rubbery state. This was deduced to be the effect of azithromycin and COL as they were crystalline, thus impacted on these two formulations to make it less amorphous.

Previous studies had shown that by spray drying azithromycin (without the addition of polymer) can turn its original crystalline structure to amorphous, with a glass transition value of around 93 °C - 95 °C. It was observed that the glass temperature decreased with the increase of pump rates during spray drying (Li *et al.* 2014b). However, in this study, endothermic peaks of spray-dried formulations were not observed, thus in agreement with the fact that azithromycin was being encapsulated in the carrier – PLGA.

3.4.6. X-ray powder diffraction (XRD)
Well-defined sharp peaks were shown in the XRD pattern of azithromycin, thus indicating the crystalline nature of azithromycin, whereas in the XRD pattern of PLGA, one broad diffusive halo at $2\theta = 20.7°$ was shown, therefore proving the amorphous nature of PLGA (Figure 5). Two broad peaks (not halo) were observed in the XRD pattern of PVA (at $2\theta = 20.06°$ and at $2\theta = 40.92°$), as the two peaks were of a combined behaviour, this matched with the DSC data which suggested that PVA was semi-crystalline and semi-amorphous. For COL, there was a low intensity broad diffusive halo at $2\theta = 22.24°$ and a high intensity well-defined sharp peak at $2\theta = 44.34°$. According to the correlation between the intensity of the peaks and the degree of crystallinity, it confirmed the results obtained in DSC that to a large extent COL was crystalline, but it was also slightly amorphous. Previous studies showed that chitosan had a rigid crystalline structure due to the formation of inter- and intromolecular hydrogen bonding owing to its hydroxyl and amine groups (Seyfarth *et al.* 2008).

Broad peaks were observed in AZI w/o and A&C w/o at $2\theta = 19°$ respectively, thus suggesting their semi-crystalline and semi-amorphous structure and that they were under the influence of PVA, whereas broad diffusion halos were observed in AZI w/ and

A&C w/ at $2\theta = 19°$ respectively, thus indicating they were amorphous and under the influence of PLGA. Since AZI w/ and A&C w/ were amorphous, they contained a flexible backbone, thus having a greater ionic diffusivity and higher ionic conductivity compared to AZI w/o and A&C w/o.

No observable well-defined sharp peaks corresponding to azithromycin were observed in all formulations, thus showing that complete or almost-complete dissolution/encapsulation of azithromycin in the polymer matrix.

3.4.7. In-vitro aerosol dispersion performance by Next Generation Impactor (NGI®)

It can be observed that in both cases (with and without centrifugation), the addition of chitosan produced a relatively low deposition of azithromycin in the inhaler and throat regions and that an increase in deposition from Stage 2 to Stage 8 was observed, thus indicating an improvement in dispersibility of the chitosan-related formulations, hence suggesting the possibilities of using COL as dispersibility enhancers.

All formulations were highly dispersible, as the emitted dose were all over 80%. The dry powder of all four formulations were suitable for pulmonary drug delivery as they all had a MMAD value, as shown in Table 3 and Figure 6, lower than 5 μm. However, the MMAD values of all formulations were significantly higher than that of their corresponding X_{50} ($p \leq 0.05$), thus suggesting the particles aggregated during aerosolisation and that they might not be optimally dispersed. Moreover, although the X_{50} and VMD of the spray-dried powder of the two formulations without centrifugation were lower than that of with centrifugation, it was shown that the formulations with centrifugation gave a better FPF, which proved better dispersibility and aerosolisation. Therefore, it can be assumed that for AZI w/o and A&C w/o, the excessive PVA act as a pressure to squeeze the particles closer together, thus resulting in a lower particle size. However, upon aerosolisation, the excessive PVA fell apart and was deposited at early stages.

Lastly, it was shown that all four formulations were able to deliver the drug to the deep lung regions, demonstrating their potential application as an effective method to treat lower respiratory tract infections such as COVID-19.

4. Conclusion

This study demonstrated the successful preparation of azithromycin-loaded PLGA nanocomposite microparticles by using double emulsion and spray drying methods. The addition of chitosan successfully altered the formulation to positively-charged nanoparticles, and was sequentially shown to enhance its dispersibility profile. Through the in-vitro aerosol dispersion performance, it was proved that formulations with centrifugation gave a better FPF, which indicated better dispersibility and aerosolisation. All dry powder formulations were able to deliver azithromycin to the deep lung regions as they all had a MMAD value lower than 5 μm, which suggested the potential of using azithromycin via pulmonary drug delivery as an effective method to treat COVID-19.

ORCID

Stefanie Ho Yi Chan http://orcid.org/0000-0002-1912-3081
Mohammed Gulrez Zariwala http://orcid.org/0000-0001-9944-8451

References

Abaleke, E., and Abbas, M., et al., 2021. Azithromycin in patients admitted to hospital with COVID-19 (RECOVERY): a randomised, controlled, open-label, platform trial. The lancet, 397 (10274), 605–612.

Al-Rimawi, F., and Kharoaf, M., 2010. Analysis of azithromycin and its related compounds by RP-HPLC with UV detection. Journal of chromatographic science, 48 (2), 86–90.

ANTICOV. 2021. An open-label, multicentre, randomised, adaptive platform trial of the safety and efficacy of several therapies, including antiviral therapies, versus control in mild/moderate cases of COVID-19. ANTICOV Master Clinical Study Protocol, 1, 1–108.

Arnold, S., 2022. Randomized, multi-arm phase II trial of novel agents for treatment of high-risk COVID-19 positive patients (clinical trial registration No. NCT04374019). https://clinicaltrials.gov/ct2/show/study/NCT04374019

Bandyopadhyaya, R., Lall, A.A., and Friedlander, S.K., 2004. Aerosol dynamics and the synthesis of fine solid particles. *Powder technology*, 139 (3), 193–199.

Barnabas, R.V., et al., 2021. Hydroxychloroquine as postexposure prophylaxis to prevent severe acute respiratory syndrome coronavirus 2 infection. *Annals of internal medicine*, 174 (3), 344–352.

Bramante, C.T., COVID-OUT Trial Team., et al., 2022. Randomized trial of metformin, ivermectin, and fluvoxamine for Covid-19. *The New England journal of medicine*, 387 (7), 599–610.

Butler, C.C., et al., 2021. Azithromycin for community treatment of suspected COVID-19 in people at increased risk of an adverse clinical course in the UK (PRINCIPLE): a randomised, controlled, open-label, adaptive platform trial. *The lancet*, 397 (10279), 1063–1074.

Cairns, D.M., et al., 2022. Efficacy of niclosamide vs placebo in SARS-CoV-2 respiratory viral clearance, viral shedding, and duration of symptoms among patients with mild to moderate COVID-19: a phase 2 randomized clinical trial. *JAMA network open*, 5 (2), e2144942.

Cavalcanti, A.B., Coalition Covid-19 Brazil I Investigators., et al., 2020. Hydroxychloroquine with or without azithromycin in mild-to-moderate Covid-19. *The New England journal of medicine*, 383 (21), 2041–2052.

Clemency, B.M., et al., 2022. Efficacy of inhaled ciclesonide for outpatient treatment of adolescents and adults with symptomatic COVID-19: a randomized clinical trial. *JAMA internal medicine*, 182 (1), 42–49.

Danhier, F., et al., 2012. PLGA-based nanoparticles: an overview of biomedical applications. *Journal of controlled release*, 161 (2), 505–522.

Dasankoppa, F., et al., 2017. Design, formulation, and evaluation of *in situ* gelling ophthalmic drug delivery system comprising anionic and nonionic polymers. *Indian journal of health sciences and biomedical research*, 10 (3), 323.

Declercq, J., et al., 2020. Zilucoplan in patients with acute hypoxic respiratory failure due to COVID-19 (ZILU-COV): a structured summary of a study protocol for a randomised controlled trial. *Trials*, 21 (1), 934.

Echeverría-Esnal, D., et al., 2021. Azithromycin in the treatment of COVID-19: a review. *Expert review of anti-infective therapy*, 19 (2), 147–163.

Eli Lilly and Company, 2022. A randomized, double-blind, placebo-controlled, phase 2 study to evaluate the efficacy and safety of mono and combination therapy with monoclonal antibodies in participants with mild to moderate COVID-19 illness (BLAZE-4) (clinical trial registration No. NCT04634409). https://clinicaltrials.gov/ct2/show/study/NCT04634409

Ezer, N., et al., 2021. Inhaled and intranasal ciclesonide for the treatment of Covid-19 in adult outpatients: CONTAIN phase II randomised controlled trial. *British medical journal*, 375, e068060.

Fonte, P., et al., 2011. Chitosan-coated solid lipid nanoparticles enhance the oral absorption of insulin. *Drug delivery and translational research*, 1 (4), 299–308.

Furtado, R.H.M., et al., 2020. Azithromycin in addition to standard of care versus standard of care alone in the treatment of patients admitted to the hospital with severe COVID-19 in Brazil (COALITION II): a randomised clinical trial. *The lancet*, 396 (10256), 959–967.

Garcia-Contreras, L., and Hickey, A.J., 2002. Pharmaceutical and biotechnological aerosols for cystic fibrosis therapy. *Advanced drug delivery reviews*, 54 (11), 1491–1504.

Gentile, P., et al., 2014. An overview of poly(lactic-co-glycolic) acid (PLGA)-based biomaterials for bone tissue engineering. *International journal of molecular sciences*, 15 (3), 3640–3659.

GlaxoSmithKline, 2022. A randomized, double-blind, placebo-controlled, study evaluating the efficacy and safety of otilimab IV in patients with severe pulmonary COVID-19 related disease (clinical trial registration No. NCT04376684). https://clinicaltrials.gov/ct2/show/study/NCT04376684

Gottlieb, R.L., GS-US-540-9012 (PINETREE) Investigators., et al., 2022. Early remdesivir to prevent progression to severe Covid-19 in outpatients. *The New England journal of medicine*, 386 (4), 305–315.

Grau, M.J., Kayser, O., and Müller, R.H., 2000. Nanosuspensions of poorly soluble drugs—reproducibility of small scale production. *International journal of pharmaceutics*, 196 (2), 155–159.

Guimarães, P.O., STOP-COVID Trial Investigators., et al., 2021. Tofacitinib in patients hospitalized with Covid-19 pneumonia. *The New England journal of medicine*, 385 (5), 406–415.

Günday Türeli, N., Türeli, A.E., and Schneider, M., 2016. Optimization of ciprofloxacin complex loaded PLGA nanoparticles for pulmonary treatment of cystic fibrosis infections: design of experiments approach. *International journal of pharmaceutics*, 515 (1–2), 343–351.

Hammond, J., EPIC-HR Investigators., et al., 2022. Oral nirmatrelvir for high-risk, nonhospitalized adults with Covid-19. *The New England journal of medicine*, 386 (15), 1397–1408.

Han, R., Papadopoulos, G., and Greenspan, B.J., 2002. Investigation of powder dispersion inside a SPIROSR dry powder inhaler using particle image velocimetry. *Powder technology*, 125 (2–3), 266–278.

Hassan, M.S. and Lau, R.W.M., 2009. Effect of particle shape on dry particle inhalation: study of flowability, aerosolization, and deposition properties. *AAPS PharmSciTech*, 10 (4), 1252–1262.

Hayes, D., Jr., et al., 2010. Aerosolized vancomycin for the treatment of MRSA after lung transplantation. *Respirology*, 15 (1), 184–186.

Hickey, A.J., et al., 2006. Inhaled azithromycin therapy. *Journal of aerosol medicine*, 19 (1), 54–60.

Hinks, T.S.C., et al., 2021. Azithromycin versus standard care in patients with mild-to-moderate COVID-19 (ATOMIC2): an open-label, randomised trial. *The lancet-respiratory medicine*, 9 (10), 1130–1140.

Hung, I.F.-N., et al., 2020. Triple combination of interferon beta-1b, lopinavir–ritonavir, and ribavirin in the treatment of patients admitted to hospital with COVID-19: an open-label, randomised, phase 2 trial. *The lancet*, 395 (10238), 1695–1704.

Kanoh, S., and Rubin, B.K., 2010. Mechanisms of action and clinical application of macrolides as immunomodulatory medications. *Clinical microbiology reviews*, 23 (3), 590–615.

Keck, C., and Muller, R., 2006. Drug nanocrystals of poorly soluble drugs produced by high pressure homogenisation. *European journal of pharmaceutics and biopharmaceutics*, 62 (1), 3–16.

Kocbek, P., Baumgartner, S., and Kristl, J., 2006. Preparation and evaluation of nanosuspensions for enhancing the dissolution of poorly soluble drugs. *International journal of pharmaceutics*, 312 (1–2), 179–186.

Kumar, V., et al., 2021. COVID-19 pandemic: mechanism, diagnosis, and treatment. *Journal of chemical technology & biotechnology*, 96 (2), 299–308.

Li, X., et al., 2014a. Design, characterization, and aerosol dispersion performance modeling of advanced co-spray dried antibiotics with mannitol as respirable microparticles/nanoparticles for targeted pulmonary delivery as dry powder inhalers. *Journal of pharmaceutical sciences*, 103 (9), 2937–2949.

Li, X., et al., 2014b. Physicochemical characterization and aerosol dispersion performance of organic solution advanced spray-dried microparticulate/nanoparticulate antibiotic dry powders of tobramycin and azithromycin for pulmonary inhalation aerosol delivery. *European journal of pharmaceutical sciences*, 52, 191–205.

Lode, H., 1991. The pharmacokinetics of azithromycin and their clinical significance. *European journal of clinical microbiology & infectious diseases*, 10 (10), 807–812.

Luke, D.R., and Foulds, G., 1997. Disposition of oral azithromycin in humans*. *Clinical pharmacology and therapeutics*, 61 (6), 641–648.

Mangal, S., et al., 2018. Physico-chemical properties, aerosolization and dissolution of co-spray dried azithromycin particles with L-leucine for inhalation. *Pharmaceutical research*, 35 (2), 28.

Mantero, V., et al., 2021. COVID-19 in dimethyl fumarate-treated patients with multiple sclerosis. *Journal of neurology*, 268 (6), 2023–2025.

McEneny-King, A.C., Monteleone, J.P.R., Kazani, S.D., and Ortiz, S.R., 2021. Pharmacokinetic and pharmacodynamic evaluation of ravulizumab in adults with severe coronavirus disease 2019. *Infectious diseases and therapy*, 10, 1045–1054.

Mittal, G., et al., 2007. Estradiol loaded PLGA nanoparticles for oral administration: Effect of polymer molecular weight and copolymer composition on release behavior *in vitro* and *in vivo*. *Journal of controlled release*, 119 (1), 77–85.

Müller, R.H., and Jacobs, C., 2002. Buparvaquone mucoadhesive nanosuspension: preparation, optimisation and long-term stability. *International journal of pharmaceutics*, 237 (1–2), 151–161.

Müller, R.H., and Peters, K., 1998. Nanosuspensions for the formulation of poorly soluble drugs. *International journal of pharmaceutics*, 160 (2), 229–237.

National Institute for Health and Care Excellence, 2022. COVID-19 rapid guideline: managing COVID-19. National Institute for Health and Care Excellence: Clinical Guideline No.191. (ISBN-13: 978-1-4731-4074-5).

National Institute of Allergy and Infectious Diseases (NIAID), 2022. A multicenter platform trial of putative therapeutics for the treatment of COVID-19 in hospitalized adults (Clinical trial registration No. NCT04583956). https://www.clinicaltrials.gov/ct2/show/study/NCT04583956

Oldenburg, C.E., et al., 2021. Effect of oral azithromycin vs. placebo on COVID-19 symptoms in outpatients with SARS-CoV-2 infection: a randomized clinical trial. *JAMA*, 326 (6), 490–498.

Oliver, M.E., and Hinks, T.S.C., 2021. Azithromycin in viral infections. *Reviews in medical virology*, 31 (2), e2163.

Perez, C., et al., 2001. Poly(lactic acid)-poly(ethylene glycol) nanoparticles as new carriers for the delivery of plasmid DNA. *J. Controlled release*, 75 (1–2), 211–224.

Profact Inc., 2022. A phase 2 screening study of candidate non-prescription treatments for COVID-19: a patient-driven, randomized, factorial study evaluating patient-reported outcomes (PROFACT-01). (Clinical trial registration no. NCT04621149). https://clinicaltrials.gov/ct2/show/study/NCT04621149

Rizzardini, G., 2020. A multi-center, randomized, double-blind, placebo-controlled, phase III clinical study evaluating the efficacy and safety of favipiravir in the treatment of patients with COVID-19-moderate type. (Clinical trial registration no. NCT04336904). https://clinicaltrials.gov/ct2/show/NCT04336904

Rogueda, P.G., and Traini, D., 2007. The nanoscale in pulmonary delivery. Part 1: deposition, fate, toxicology and effects. *Expert opinion on drug delivery*, 4 (6), 595–606.

Ruan, X., et al., 2022. Remdesivir powders manufactured by jet milling for potential pulmonary treatment of COVID-19. *Pharmaceutical development and technology*, 27 (6), 635–645.

Sahakijpijarn, S., et al., 2020. Development of remdesivir as a dry powder for inhalation by thin film freezing. *Pharmaceutics*, 12 (11), 1002.

Santoro, F., et al., 2022. Antiplatelet therapy and outcome in COVID-19: the health outcome predictive evaluation registry. *Heart*, 108 (2), 130–136.

Sekhavati, E., et al., 2020. Safety and effectiveness of azithromycin in patients with COVID-19: an open-label randomised trial. *International journal of antimicrobial agents*, 56 (4), 106143.

Seyfarth, F., et al., 2008. Antifungal effect of high- and low-molecular-weight chitosan hydrochloride, carboxymethyl chitosan, chitosan oligosaccharide and N-acetyl-d-glucosamine against *Candida albicans*, *Candida krusei* and *Candida glabrata*. *International journal of pharmaceutics*, 353 (1–2), 139–148.

Sharma, S., et al., 2016. PLGA-based nanoparticles: a new paradigm in biomedical applications. *TrAC trends in analytical chemistry*, 80, 30–40.

Shoumann, W.M., et al., 2021. Use of ivermectin as a potential chemoprophylaxis for COVID-19 in Egypt: a randomised clinical trial. *Journal of clinical and diagnostic research*, 15 (2), OC27–OC32.

Sun, D., 2020. Remdesivir for treatment of COVID-19: combination of pulmonary and IV administration may offer adittional benefit. *The AAPS journal*, 22 (4), 77.

The COVID STEROID 2 Trial Group, 2021. Effect of 12 mg vs 6 mg of dexamethasone on the number of days alive without life support in adults with COVID-19 and severe hypoxemia: the COVID steroid 2 randomized trial. *JAMA*, 326 (18), 1807–1817.

The RECOVERY Collaborative Group, 2021. Dexamethasone in hospitalized patients with Covid-19. *New England journal of medicine*, 384 (8), 693–704.

Touret, F., et al., 2020. *In vitro* screening of a FDA approved chemical library reveals potential inhibitors of SARS-CoV-2 replication. *Scientific reports*, 10 (1), 13093.

Wilkinson, T., *et al*., 2020. ACCORD: a multicentre, seamless, phase 2 adaptive randomisation platform study to assess the efficacy and safety of multiple candidate agents for the treatment of COVID-19 in hospitalised patients: a structured summary of a study protocol for a randomised controlled trial. *Trials*, 21 (1), 691.

University of Dundee, 2021. A randomised double-blind placebo-controlled trial of brensocatib (INS1007) in patients with severe COVID-19 (Clinical trial registration No. NCT04817332). https://clinicaltrials.gov/ct2/show/study/NCT04817332

Smieszek, S.P., *et al*., 2021. Assessing the potential correlation of polymorphisms in the IL6R with relative IL6 elevation in severely ill COVID-19 patients'. *Cytokine*, 148, 155662.

Vartak, R., *et al*., 2021. Aerosolized nanoliposomal carrier of remdesivir: an effective alternative for COVID-19 treatment *in vitro*. *Nanomedicine*, 16 (14), 1187–1202.

Young, P.M., *et al*., 2015. Multi-breath dry powder inhaler for delivery of cohesive powders in the treatment of bronchiectasis. *Drug development and industrial pharmacy*, 41 (5), 859–865.